



This is a repository copy of *Review: Defect chemistry and electrical properties of sodium bismuth titanate perovskite*.

White Rose Research Online URL for this paper:  
<http://eprints.whiterose.ac.uk/124635/>

Version: Accepted Version

---

**Article:**

Yang, F. [orcid.org/0000-0002-6428-7755](https://orcid.org/0000-0002-6428-7755), Li, M., Li, L. et al. (3 more authors) (2017)  
Review: Defect chemistry and electrical properties of sodium bismuth titanate perovskite.  
Journal of Materials Chemistry A, 13 (6). 5243-5254 . ISSN 2050-7488

<https://doi.org/10.1039/C7TA09245H>

---

**Reuse**

Items deposited in White Rose Research Online are protected by copyright, with all rights reserved unless indicated otherwise. They may be downloaded and/or printed for private study, or other acts as permitted by national copyright laws. The publisher or other rights holders may allow further reproduction and re-use of the full text version. This is indicated by the licence information on the White Rose Research Online record for the item.

**Takedown**

If you consider content in White Rose Research Online to be in breach of UK law, please notify us by emailing [eprints@whiterose.ac.uk](mailto:eprints@whiterose.ac.uk) including the URL of the record and the reason for the withdrawal request.



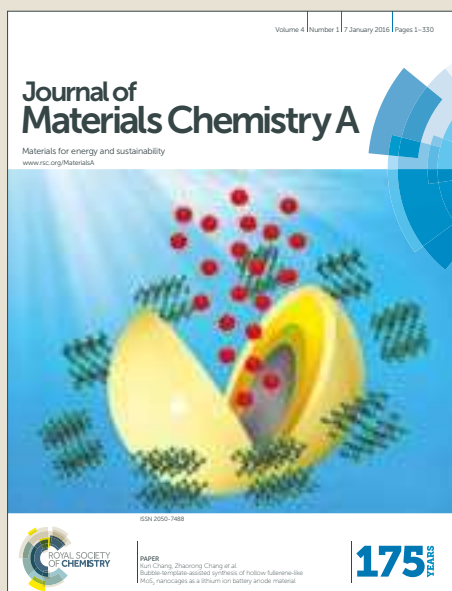
[eprints@whiterose.ac.uk](mailto:eprints@whiterose.ac.uk)  
<https://eprints.whiterose.ac.uk/>

# Journal of Materials Chemistry A

Accepted Manuscript



This article can be cited before page numbers have been issued, to do this please use: F. Yang, M. Li, L. Li, P. Wu, E. Pradal-Velázquez and D. Sinclair, *J. Mater. Chem. A*, 2017, DOI: 10.1039/C7TA09245H.



This is an Accepted Manuscript, which has been through the Royal Society of Chemistry peer review process and has been accepted for publication.

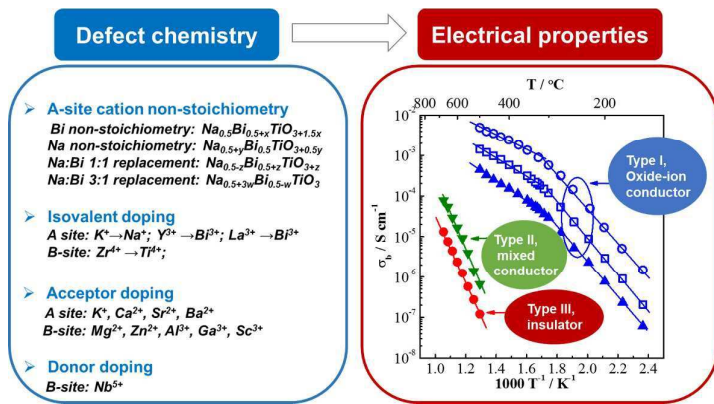
Accepted Manuscripts are published online shortly after acceptance, before technical editing, formatting and proof reading. Using this free service, authors can make their results available to the community, in citable form, before we publish the edited article. We will replace this Accepted Manuscript with the edited and formatted Advance Article as soon as it is available.

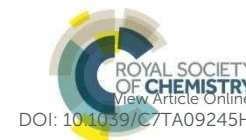
You can find more information about Accepted Manuscripts in the [author guidelines](#).

Please note that technical editing may introduce minor changes to the text and/or graphics, which may alter content. The journal's standard [Terms & Conditions](#) and the ethical guidelines, outlined in our [author and reviewer resource centre](#), still apply. In no event shall the Royal Society of Chemistry be held responsible for any errors or omissions in this Accepted Manuscript or any consequences arising from the use of any information it contains.

## Table of contents entry

We review the diversity of electrical behaviour of NBT induced by various defect mechanisms, including A-site Na or Bi non-stoichiometry, isovalent-, acceptor- and donor-doping.





Journal Name

ARTICLE

## Review: Defect chemistry and electrical properties of sodium bismuth titanate perovskite

F. Yang,<sup>\*a</sup> M. Li,<sup>b</sup> L. Li,<sup>a</sup> P. Wu,<sup>a</sup> E. Pradal-Velázquez<sup>a</sup> and D. C. Sinclair<sup>\*a</sup>Received 00th January 20xx,  
Accepted 00th January 20xx

DOI: 10.1039/x0xx00000x

[www.rsc.org/](http://www.rsc.org/)

The ferroelectric perovskite  $\text{Na}_{0.5}\text{Bi}_{0.5}\text{TiO}_3$ , NBT, can exhibit three types of electrical behaviour, i.e. oxide-ion conduction (Type I), mixed ionic-electronic conduction (Type II) and insulating/dielectric (Type III) based on various defect mechanisms. Here we review how to tune the electrical properties of NBT via several mechanisms, including A-site Na or Bi non-stoichiometry, isovalent substitution, acceptor- and donor-doping. The diversity of electrical behaviour in the NBT lattice is attributed to the high level of oxide-ion conductivity originating from highly mobile oxygen ions which can be fine-tuned to optimise or suppress the ionic conduction. High oxide-ion conductivity can be obtained by manipulating the starting Na/Bi  $\geq 1$  and by acceptor-doping to make NBT a potential electrolyte material for intermediate temperature solid oxide fuel cells (IT-SOFCs). In contrast, the oxide-ion conduction can be partially or fully suppressed by having a starting (nominal) composition with Na/Bi  $< 1$ , donor-doping, or utilising the trapping between oxygen vacancies and some B-site acceptor dopants. This significantly reduces the dielectric loss and makes NBT-based materials excellent candidates as high-temperature dielectrics for capacitor applications.

### Introduction

Sodium bismuth titanate,  $\text{Na}_{0.5}\text{Bi}_{0.5}\text{TiO}_3$  (NBT), is considered as one of the most promising lead-free piezoelectric materials to replace lead zirconate titanate (PZT) because of its high Curie temperature ( $\sim 325$  °C), relatively high remnant polarization ( $38 \mu\text{C cm}^{-2}$ ) and piezoelectric constant ( $73 \text{ pC N}^{-1}$ ).<sup>1-3</sup> NBT was first reported in the 1960s and has received increasing attention in recent years driven by the surge in developing lead-free materials.<sup>4</sup> There has been extensive research on the crystal structure and phase transformation of NBT<sup>5-10</sup>, and numerous efforts have been devoted to improving its piezoelectric properties.<sup>4, 11-20</sup>

One major drawback of NBT as a piezoelectric/dielectric material is its high electrical conductivity which leads to high and unacceptable dielectric loss and leakage currents at elevated temperatures.<sup>1</sup> To solve this problem improved understanding of the electrical conductivity and the conduction mechanism(s) of NBT is essential. Hiruma *et al.*<sup>21</sup> and Sung *et al.*<sup>22, 23</sup> have shown the electrical properties of NBT are highly sensitive to A-site cation nonstoichiometry and that small deviations in nominal A-site cation stoichiometry can result in more than 3 orders of magnitude difference in the room temperature dc resistivity. Although it is widely accepted that the mobility of oxygen vacancies plays an important role<sup>22, 23</sup> and that  $\text{Bi}_2\text{O}_3$  loss during ceramic processing is a likely source of the oxygen vacancies<sup>21, 22, 24</sup>, the origin of the dramatic dependence of electrical conductivity with such small

variations in the nominal starting compositions, as well as the conduction mechanism(s) of NBT, remain challenging issues.

Recently, we used a combination of impedance spectroscopy, electromotive force (EMF) and  $^{18}\text{O}$  Time-of-Flight Secondary Ion Mass Spectroscopy (ToF SIMS) to clarify the electrical conduction mechanisms in NBT and revealed the significant change in the electrical conductivity induced by small variations of Na or Bi nonstoichiometry being related to a switch between oxide-ion and electronic conduction.<sup>25, 26</sup> The nominally stoichiometric NBT (nominal  $\text{Na}_{0.5}\text{Bi}_{0.5}\text{TiO}_3$ ;  $\text{NB}_{0.50}\text{T}$ ), presents high conductivity with an oxide-ion transport number  $t_{\text{ion}} \sim 0.9$  at 600 - 800 °C, suggesting the electrical conduction is dominated by oxide-ions. The predominance of oxide-ion conduction (as opposed to sodium ion or electronic conduction) in  $\text{NB}_{0.50}\text{T}$  has been further confirmed by  $^{18}\text{O}$  tracer diffusion measurements. The high oxide-ion conductivity in  $\text{NB}_{0.50}\text{T}$  is attributed to oxygen vacancies generated through low levels of  $\text{Bi}_2\text{O}_3$  loss during ceramic processing according to the Kroger-Vink equation,



as well as the high oxygen ion mobility associated with highly polarized  $\text{Bi}^{3+}$  ions and weak Bi-O bonds.<sup>27</sup> Higher oxide-ion conductivity is achieved in Bi-deficient NBT (nominal  $\text{Na}_{0.5}\text{Bi}_{0.49}\text{TiO}_{2.985}$ ;  $\text{NB}_{0.49}\text{T}$ ) due to generation of additional oxygen vacancies. In contrast, the oxide-ion conductivity is suppressed in Bi-excess NBT (nominal  $\text{Na}_{0.5}\text{Bi}_{0.51}\text{TiO}_{3.015}$ ;  $\text{NB}_{0.51}\text{T}$ ) as the excess  $\text{Bi}_2\text{O}_3$  in  $\text{NB}_{0.51}\text{T}$  can compensate for the loss during processing, thus  $\text{NB}_{0.51}\text{T}$  exhibits electronic conduction with an activation energy of  $\sim 1.6$  eV which is close to half of the band gap of NBT.<sup>28</sup> The predominant electronic conduction in  $\text{NB}_{0.51}\text{T}$  is confirmed by a  $t_{\text{ion}} < 0.1$  at 600 - 800 °C. Interestingly, later work shows a further increase in the starting Bi-excess content (for example,  $\text{Na}_{0.5}\text{Bi}_{0.52}\text{TiO}_{3.03}$ ;  $\text{NB}_{0.52}\text{T}$ ) can reintroduce significant levels of oxide-ion conductivity into NBT.  $\text{NB}_{0.52}\text{T}$  shows mixed conduction behaviour with comparable contributions from oxide-ion and electronic conduction showing a

<sup>a</sup> Department of Materials Science & Engineering, University of Sheffield, Sheffield, S1 3JD, UK. Email: [fan.yang@sheffield.ac.uk](mailto:fan.yang@sheffield.ac.uk); [d.c.sinclair@sheffield.ac.uk](mailto:d.c.sinclair@sheffield.ac.uk)

<sup>b</sup> Department of Mechanical, Materials and Manufacturing Engineering, University of Nottingham, NG7 2RD, UK.

$t_{\text{ion}}$  close to 0.5, which is possibly linked to a change in the Bi-content in the NBT main phase or a space charge effect because of the presence of Bi-rich secondary phase.<sup>29</sup>

Based on the magnitude of bulk conductivity,  $\sigma_b$  and  $t_{\text{ion}}$  values, we have concluded that NBT can exhibit three types of electrical behaviour by tailoring the A-site Na/Bi non-stoichiometry (Fig.1a): Type I, predominant oxide-ion conduction, high  $\sigma_b$ ,  $t_{\text{ion}} \sim 0.9$ ; Type II, mixed ionic-electronic conduction, intermediate  $\sigma_b$ ,  $t_{\text{ion}} \sim 0.5$ ; Type III, predominant electronic conduction, low  $\sigma_b$ ,  $t_{\text{ion}} < 0.1$ . These three types of electrical behaviour can also be clearly distinguished from the  $\tan \delta - T$  relationship, Fig.1b. Type I NBT shows a sharp rise of  $\tan \delta$  with increasing temperature and  $\tan \delta$  exceeds 0.2 at  $\sim 350$  °C. In contrast, Type III NBT presents low  $\tan \delta$  in a wide temperature range ( $< 0.02$  from 300 to 600 °C), making it an excellent high temperature dielectric material. In between Type I and III, Type II shows low  $\tan \delta$  in a narrow temperature range and a steep rise above  $\sim 500$  °C to exceed 0.1 at 600 °C.

The above findings not only reveal the electrical conduction behaviour of NBT but also show the flexibility in tailoring the electrical conductivity and conduction mechanisms in NBT and expand the potential application of NBT-based materials from piezoelectric/dielectric devices to oxide-ion and mixed ionic-electronic conductors. They also highlight the importance of defect chemistry on the electrical properties of NBT. Here we review how to tune the electrical properties of NBT by various defect mechanisms including; A-site Na or Bi non-stoichiometry; isovalent substitution; acceptor- and donor-doping. In particular, we focus on controlling the oxide-ion conduction in NBT to switch the conduction mechanism and conductivity among Types I, II and III according to the requirements for different applications.

The structure of this review is as follows. First, we review the defect chemistry and electrical properties of undoped NBT, which consists only of Na, Bi, Ti and O without any other dopant and therefore rules out any possible influence from foreign ions. Second, results from isovalent doping which does not introduce any oxygen vacancies into NBT are discussed to unveil the important parameters that may affect oxide-ion conduction in NBT. Third, possible compensation mechanism(s) from acceptor-doping in NBT are discussed with an attempt to enhance the bulk conductivity and to explore the potential of NBT-based materials as electrolytes in IT-SOFCs. We also demonstrate the possibility of suppressing the oxide-ion conduction in NBT using the trapping effect between B-site acceptor-dopants and oxygen vacancies. Finally, the influence of donor-doping on the electrical properties are reviewed to demonstrate dielectric/insulating behaviour thus rendering NBT-based materials as potential candidates for high temperature dielectric/piezoelectric applications. The article concludes with a summary to highlight the important findings, to date.

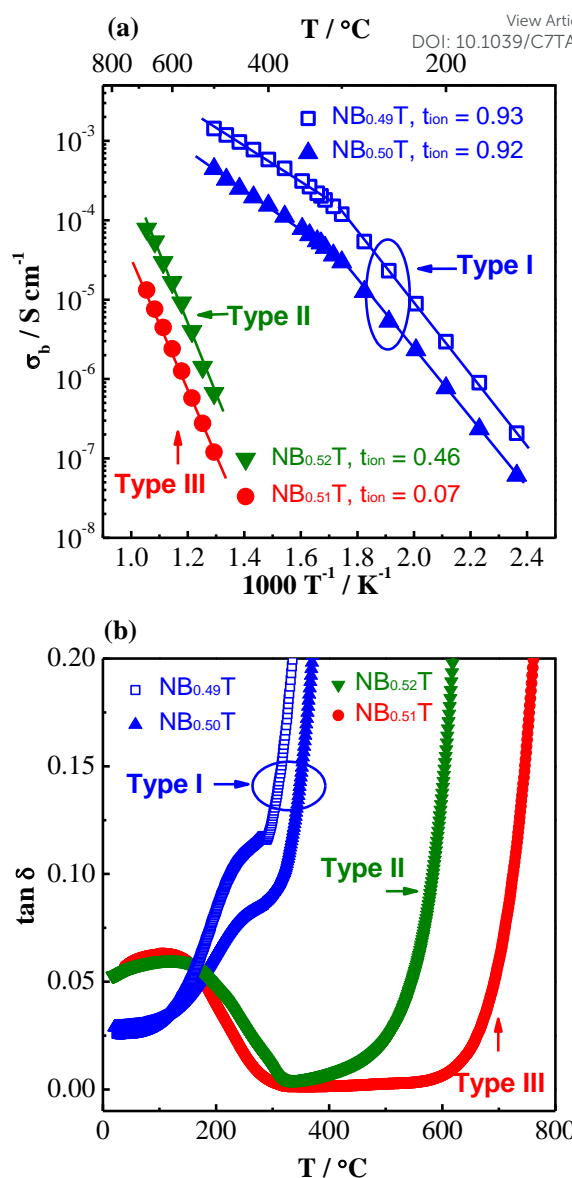


Fig.1 (a) Arrhenius plot of bulk conductivity,  $\sigma_b$  and (b) dielectric loss,  $\tan \delta$ , at 1 MHz versus temperature for NBT with various A-site Bi nonstoichiometry:  $\text{Na}_{0.5}\text{Bi}_{0.49}\text{TiO}_{2.985}$ ,  $\text{NB}_{0.49}\text{T}$ ;  $\text{Na}_{0.5}\text{Bi}_{0.5}\text{TiO}_3$ ,  $\text{NB}_{0.50}\text{T}$ ;  $\text{Na}_{0.5}\text{Bi}_{0.51}\text{TiO}_{3.015}$ ,  $\text{NB}_{0.51}\text{T}$ ;  $\text{Na}_{0.5}\text{Bi}_{0.52}\text{TiO}_{3.03}$ ,  $\text{NB}_{0.52}\text{T}$ . Replotted after ref.29.

## Defect chemistry and electrical properties of NBT

### Undoped NBT

Our earlier studies<sup>25, 26</sup> showed the electrical conductivity and conduction mechanisms are highly sensitive to the A-site Na or Bi non-stoichiometry. For nominal Na/Bi ratios  $\geq 1$ , NBT exhibits high oxide-ion conductivity; nominal Na/Bi ratios  $< 1$  dramatically suppress the oxide-ion conduction and 'switch' NBT to a predominant  $n$ -type electronic semiconductor/insulator. In recent follow-on studies, three different mechanisms were employed to manipulate the A-site Na or Bi non-stoichiometry in attempts to fully establish the mechanism(s) and levels of nonstoichiometry in NBT

and to improve our understanding of the oxide-ion conducting to semiconducting/insulating switch over.

First, we investigated finer increments of A-site non-stoichiometry with two series of materials, Bi non-stoichiometry based on the general formula  $\text{Na}_{0.5}\text{Bi}_{0.5+x}\text{TiO}_{3+1.5x}$  ( $x = -0.02, -0.01, -0.005, 0, 0.005, 0.01, 0.02$  and  $0.05$ ) and Na non-stoichiometry based on  $\text{Na}_{0.5+y}\text{Bi}_{0.5}\text{TiO}_{3+0.5y}$  ( $y = -0.01, 0$  and  $0.01$ ). The phase purity and the electrical properties in these ceramics were examined using various techniques. Second, a Na:Bi 1:1 substitution mechanism ( $\text{Na}^+ \rightarrow \text{Bi}^{3+}$ ) based on  $\text{Na}_{0.5-z}\text{Bi}_{0.5+z}\text{TiO}_{3+z}$  ( $z = -0.02, -0.01, 0, 0.01, 0.02$ ) was studied. This substitution mechanism aimed to alter the Na/Bi ratio while maintaining the A-site of the perovskite to be fully occupied. Third, a Na: Bi 3:1 substitution mechanism ( $3\text{Na}^+ \rightarrow \text{Bi}^{3+}$ ) based on  $\text{Na}_{0.5+3w}\text{Bi}_{0.5-w}\text{TiO}_3$  ( $w = -0.05, -0.02, -0.01, 0, 0.05$ ) was investigated. This mechanism maintains A-site charge neutrality without introducing any oxygen deficiency. Results of the above three non-stoichiometry mechanisms are summarised in this section.

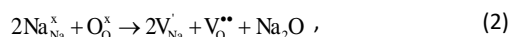
### Bi or Na non-stoichiometry

#### 1) Bi non-stoichiometry $\text{Na}_{0.5}\text{Bi}_{0.5+x}\text{TiO}_{3+1.5x}$ <sup>26, 29, 30</sup>

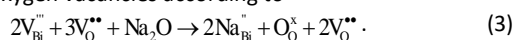
The electrical behaviour of the  $\text{Na}_{0.5}\text{Bi}_{0.5+x}\text{TiO}_{3+1.5x}$  series is summarised in Table 1. Consistent with previous studies, nominally stoichiometric ( $x = 0$ ) and Bi-deficient ( $x < 0$ ) NBTs show oxide-ion conduction behaviour (Type I), slightly Bi-excess ( $0 < x \leq 0.01$ ) NBTs show predominant electronic conduction (Type III) and more Bi-excess ( $x \geq 0.02$ ) NBTs present mixed ionic-electronic conduction (Type II). The defect mechanisms for such electrical behaviour induced by Bi non-stoichiometry are described by Equation (1) and explained in the introduction section. What should be stressed here is that the Bi non-stoichiometry level is extremely limited in NBT, as also listed in Table 1.  $\text{Na}_2\text{Ti}_6\text{O}_{13}$  and  $\text{TiO}_2$  secondary phases appear in Type I NBT whereas  $\text{Na}_{0.5}\text{Bi}_{4.5}\text{Ti}_4\text{O}_{15}$  and  $\text{Bi}_2\text{O}_3$  appear as secondary phases in Type III NBT. Among all the compositions,  $x = 0.005$  is the only one that remains single phase under the inspection of TEM. These results demonstrate (at least under our processing conditions) that single phase NBT can only be obtained with a small Bi-excess in the starting material to compensate for Bi-loss during process. It should be stressed that the level of Bi-excess required to obtain single phase NBT will be dependent on the ceramic processing conditions such as the sintering temperature/time and the use of sacrificial powder to protect ceramics during sintering.

#### 2) Na non-stoichiometry $\text{Na}_{0.5+y}\text{Bi}_{0.5}\text{TiO}_{3+0.5y}$

NBTs with Na non-stoichiometry behave in the opposite way compared to those with Bi non-stoichiometry. As also shown in Table 1, Na-deficient NBT is insulating (similar to Bi-excess in Bi non-stoichiometric NBT) and Na-rich NBT is conducting (similar to Bi-deficient in Bi non-stoichiometric NBT). For Na-deficient NBT ( $y < 0$ ), if the defect mechanism is via generating oxygen vacancies according to



it should be more ionically conductive than stoichiometric NBT ( $y = 0$ ) because of the creation of oxygen vacancies. In contrast, Na-rich NBT ( $y > 0$ ) should exhibit lower conductivity than stoichiometric NBT as the excess Na should fill the Bi vacancies and lead to partial elimination of oxygen vacancies according to



However, the observed electrical properties of the NBT series with Na non-stoichiometry are not consistent with equations (2) and (3), therefore suggesting these mechanisms are inappropriate for this series.

XRD, SEM and TEM analysis on Na non-stoichiometric NBT reveals the observed electrical behaviour originates from changes in the composition of the main phase in these ceramics. For example, for Na-deficient NBT, i.e.,  $y = -0.01$ , STEM HAADF Z-contrast images revealed the presence of  $\text{TiO}_2$  secondary phase. Thus the bulk composition is deficient in both Na and Ti, and therefore the chemical formula  $\text{Na}_{0.49}\text{Bi}_{0.50}\text{TiO}_{2.99}$  can be rewritten as  $\text{Na}_{0.5}\text{Bi}_{0.51}\text{Ti}_{1.02-6}\text{O}_{3.055-26}$  where  $\delta\text{TiO}_2$  is the secondary phase observed by TEM. Therefore, the bulk composition of  $y = -0.01$  was essentially Bi-rich to make NBT insulating (Type III). For Na-rich NBT, a Na-rich secondary phase was detected under SEM, indicating the excess Na in the starting material does not enter into the lattice. The bulk composition is Bi-deficient due to the Bi-loss during ceramic processing. Consequently, oxygen vacancies are generated according to Equation (1) and make NBT oxide-ion conducting (Type I).

#### $\text{Na}^+ \rightarrow \text{Bi}^{3+}$ <sup>31</sup>

As Na or Bi deficiency will introduce vacancies on the A-site, a Na:Bi 1:1 substitution mechanism ( $\text{Na}^+ \rightarrow \text{Bi}^{3+}$ ) with nominal composition of  $\text{Na}_{0.5-z}\text{Bi}_{0.5+z}\text{TiO}_{3+z}$  ( $z = -0.02, -0.01, 0, 0.01, 0.02$ ), which maintains the A-site of the perovskite lattice being fully occupied, was investigated. The phase purity and electrical behaviour of this series are summarised in Table 2.

With this defect mechanism, single phase NBT (based on SEM) can be obtained for  $-0.01 \leq z \leq 0.01$ .  $\text{Na}_2\text{Ti}_3\text{O}_7$  secondary phase was detected for  $z = -0.02$  and  $\text{Na}_{0.5}\text{Bi}_{4.5}\text{Ti}_4\text{O}_{15}$  secondary phase was detected for  $z = 0.02$ . Similar to Na or Bi non-stoichiometry, NBT also exhibits Type I behaviour with starting Na/Bi ratios  $\geq 1$  and Type III with Na/Bi ratios  $< 1$ .

The effect of Na:Bi 1:1 substitution on the electrical conduction behaviour is similar to Bi-deficient NBT where oxygen vacancies are generated to induce oxide-ion conduction (for  $z < 0$ ) or Bi-rich NBT where oxygen vacancies are filled to exhibit n-type semi-conduction (for  $z > 0$ ). As this defect mechanism does not introduce any A-site vacancies, it confirms the importance of oxygen vacancies (as opposed to the A-site cation vacancies) on the electrical conduction of NBT.

#### $3\text{Na}^+ \rightarrow \text{Bi}^{3+}$ <sup>32</sup>

A Na: Bi 3:1 substitution mechanism ( $3\text{Na}^+ \rightarrow \text{Bi}^{3+}$ ) with nominal composition of  $\text{Na}_{0.5+3w}\text{Bi}_{0.5-w}\text{TiO}_3$  ( $w = -0.05, 0, 0.01, 0.02, 0.05$ ) has also been investigated. This mechanism maintains neutral charge at the A-site without introducing any oxygen deficiency. The phase purity and electrical behaviour of this series are summarised in Table 3.

Based on XRD, large amounts of  $\text{Bi}_4\text{Ti}_3\text{O}_{12}$  can be detected for  $w = -0.05$  and a small amount of Na-rich secondary phase for  $w = 0.05$ . Phase pure NBT is only obtained for  $w = 0.01$  based on XRD. However, according to the nominal composition of  $w = 0.01$ , A-site occupancy is  $> 1$ , which is unlikely to happen. Normalising the A-site occupancy to 1 gives the formula  $\text{Na}_{0.52}\text{Bi}_{0.48}\text{Ti}_{0.98}\text{O}_{2.94}$  and would therefore generate a Na,Ti-rich secondary phase that has not been detected by XRD.

These results suggest this substitution mechanism does not yield an extensive single phase NBT solid solution. NBT with  $w > 0$  exhibits Type I behaviour which is a result of Bi-deficient bulk NBT with the presence of a Na,Ti-rich secondary phase.

### Summary

In this section, three different A-site defect mechanisms have been applied to NBT and their effects on the electrical properties are summarised in Fig. 2. In general, NBTs with Na/Bi ratios  $\geq 1$  exhibit high oxide-ion conductivity (Type I) and those with Na/Bi ratios  $< 1$  show low conductivity which is dominated by low levels of electronic

conduction (Type III). NBTs with significant levels of Bi-rich secondary phases can present mixed-conduction with comparable contributions from electronic and oxide-ion conduction (Type II). It should be stressed that the level of allowed non-stoichiometry within NBT is extremely low, usually below the detection limit of most readily available analytical methods. But such low levels of non-stoichiometry can result in more than three orders of magnitude difference in the bulk conductivity, therefore electrical measurements are the most sensitive and reliable method to detect the predominant type of non-stoichiometry in NBT.

Table 1. Electrical behaviour and phase purity of NBT with Bi and Na non-stoichiometry:  $\text{Na}_{0.5}\text{Bi}_{0.5+x}\text{TiO}_{3+1.5x}$  and  $\text{Na}_{0.5+y}\text{Bi}_{0.5}\text{TiO}_{3+0.5y}$ . Electrical behaviour, Types I, II and III, represent predominant oxide-ion conduction, mixed ionic-electronic conduction and predominant (low level) electronic conduction, respectively.

Nonstoichiometry	x or y	Na/Bi	Electrical behaviour	Phase purity			
				XRD	SEM	TEM	
Bi	-0.02	1.04	I	$\text{Na}_2\text{Ti}_6\text{O}_{13}$	$\text{Na}_2\text{Ti}_6\text{O}_{13}$	--	
	-0.01	1.02	I	clean	$\text{Na}_2\text{Ti}_6\text{O}_{13}$	$\text{TiO}_2$	
	$\text{Na}_{0.5}\text{Bi}_{0.5+x}\text{TiO}_{3+1.5x}$	-0.005	1.01	I	clean	$\text{Na}_2\text{Ti}_6\text{O}_{13}$	$\text{TiO}_2$
		0	1.00	I	clean	clean	$\text{TiO}_2$
		0.005	0.99	III	clean	clean	clean
		0.01	0.98	III	clean	clean	$\text{Bi}_2\text{O}_3$
		0.02	0.96	II	clean	clean	$\text{Bi}_2\text{O}_3$
0.05	0.91	II	$\text{Bi}_2\text{O}_3, \text{Na}_{0.5}\text{Bi}_{4.5}\text{Ti}_4\text{O}_{15}$	$\text{Bi}_2\text{O}_3, \text{Na}_{0.5}\text{Bi}_{4.5}\text{Ti}_4\text{O}_{15}$	$\text{Bi}_2\text{O}_3$		
Na	-0.01	0.98	III	clean	clean	$\text{TiO}_2$	
	0	1.00	I	clean	clean	$\text{TiO}_2$	
	$\text{Na}_{0.5+y}\text{Bi}_{0.5}\text{TiO}_{3+0.5y}$	1.02	I	clean	Na-rich phase	--	

Table 2. Phase purity and electrical behaviour of NBT with Na:Bi 1:1 substitution:  $\text{Na}_{0.5-z}\text{Bi}_{0.5+z}\text{TiO}_{3+z}$  ( $z = -0.02, -0.01, 0, 0.01, 0.02$ ).

z	Nominal composition	Na/Bi	Electrical behaviour	Phase purity	
				XRD	SEM
-0.02	$\text{Na}_{0.52}\text{Bi}_{0.48}\text{TiO}_{2.98}$	1.08	I	clean	$\text{Na}_2\text{Ti}_3\text{O}_7$
-0.01	$\text{Na}_{0.51}\text{Bi}_{0.49}\text{TiO}_{2.99}$	1.04	I	clean	clean
0	$\text{Na}_{0.5}\text{Bi}_{0.5}\text{TiO}_3$	1.00	I	clean	clean
0.01	$\text{Na}_{0.49}\text{Bi}_{0.51}\text{TiO}_{3.01}$	0.96	III	clean	clean
0.02	$\text{Na}_{0.48}\text{Bi}_{0.52}\text{TiO}_{3.02}$	0.92	III	$\text{Na}_{0.5}\text{Bi}_{4.5}\text{Ti}_4\text{O}_{15}$	$\text{Na}_{0.5}\text{Bi}_{4.5}\text{Ti}_4\text{O}_{15}$

Table 3. Phase purity and electrical behaviour of NBT with Na:Bi 3:1 substitution:  $\text{Na}_{0.5+3w}\text{Bi}_{0.5-w}\text{TiO}_3$  ( $w = -0.05, -0.02, -0.01, 0, 0.05$ ).

w	Nominal composition	Na/Bi	Electrical behaviour	Phase purity
				XRD
-0.05	$\text{Na}_{0.35}\text{Bi}_{0.55}\text{TiO}_3$	0.63	-	NBT + $\text{Bi}_4\text{Ti}_3\text{O}_{12}$
0	$\text{Na}_{0.5}\text{Bi}_{0.5}\text{TiO}_3$	1.00	I	clean
0.01	$\text{Na}_{0.53}\text{Bi}_{0.49}\text{TiO}_3$	1.08	I	clean
0.02	$\text{Na}_{0.56}\text{Bi}_{0.48}\text{TiO}_3$	1.17	I	Na-rich phase
0.05	$\text{Na}_{0.65}\text{Bi}_{0.45}\text{TiO}_3$	1.44	I	Na-rich phase

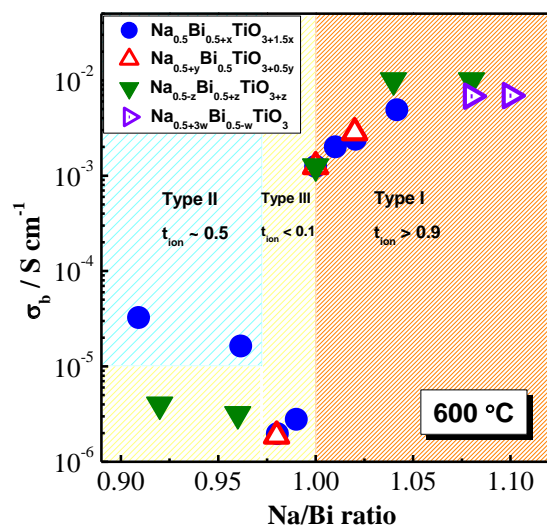


Fig. 2 Bulk conductivity of NBT at 600 °C with various Na/Bi ratios.

### Isovalent doping<sup>33</sup>

Nominally stoichiometric NBT exhibits high oxide-ion conductivity, which originates from the oxygen vacancies generated through a small amount of  $\text{Bi}_2\text{O}_3$  loss during ceramic processing. A previous study<sup>34</sup> showed that 0.5 – 1 at.% Nb doping on the B-site can fill up the oxygen vacancies and significantly decrease the electrical conductivity. Therefore, the bismuth and oxygen nonstoichiometry in NBT can be estimated to be in the range of 0.0017-0.0033 for Bi and 0.0025-0.005 for oxygen, corresponding to a formula of  $\text{Na}_{0.5}\text{Bi}_{0.4967-0.4983}\text{TiO}_{2.995-2.9975}$ .<sup>34</sup> The fact that such a low level of oxygen vacancy concentration can result in such high oxide-ion conductivity implies the mobility of oxygen ions in NBT is very high. In perovskites, the oxygen ion migration is through a saddle point which is a triangle formed by two A-site cations and one B-site cation.<sup>35</sup> In NBT, first-principles calculations<sup>36, 37</sup> showed the lowest energy barriers for oxygen ion migration occur in saddle points between Bi-Bi-Ti ions (0.22 eV), whereas higher barriers are observed for Na-Bi-Ti (0.6 – 0.85 eV) and Na-Na-Ti (1.0 - 1.3 eV) saddle points, as shown in Fig. 3. Experimentally, there is no evidence for long-range ordering of the A-site cations in NBT, therefore the Na-Bi-Ti saddle points are considered as the rate-limiting step in the overall oxide-ion migration in NBT. It is generally accepted that the high polarisability of  $\text{Bi}^{3+}$  and weak Bi-O bonds on the A-site are critical to the high mobility of oxygen ions.<sup>27</sup>

To further understand the local configuration and properties of cations on the oxide-ion conduction in NBT, isovalent doping, such as  $\text{K}^+$  to replace  $\text{Na}^+$ ,  $\text{Y}^{3+}$  or  $\text{La}^{3+}$  to replace  $\text{Bi}^{3+}$  and  $\text{Zr}^{4+}$  to replace  $\text{Ti}^{4+}$ , have been carried out. The Arrhenius plot of bulk conductivity,  $\sigma_b$ , of K-doped, Y-doped, La-doped and Zr-doped NBT obtained from impedance spectroscopy is shown in Fig. 4. The ionic radius, polarisability and bonding strength with oxygen of these elements are listed in Table 4.

Partial replacement of  $\text{Na}^+$  by  $\text{K}^+$  significantly decreases the bulk conductivity, which is surprising as  $\text{K}^+$  has higher polarisability and weaker bonding strength with oxygen compared to  $\text{Na}^+$ , which

should be beneficial for oxide-ion conduction. Here the suppressed conductivity is attributed to compositional variations associated with the higher volatility of K compared to Na. The K loss is more significant than Bi-loss during sintering, and therefore makes KNBT Bi-rich on the A-site. Partial replacement of  $\text{Bi}^{3+}$  by  $\text{Y}^{3+}$  or  $\text{La}^{3+}$  on the A-site decreases the bulk conductivity of NBT, which can be attributed to the lower polarisability of Y and La compared to Bi, as well as the much stronger Y-O or La-O bond compared to the Bi-O bond. Although the polarisability of Zr is higher than Ti, partial replacement of  $\text{Ti}^{4+}$  by  $\text{Zr}^{4+}$  also decreases the bulk conductivity of NBT, which suggests the bonding strength with oxygen plays a key role in the oxide-ion migration. The high cation-oxygen bond strength limits the mobility of oxygen ions in NBT and therefore suppresses the oxide-ion conduction. It can be predicted that these isovalent doped NBTs have much lower dielectric loss and can be excellent high-temperature dielectric materials with appropriate doping levels.



Fig. 3 Saddle-point configuration and associated activation energies for oxygen ion migration in NBT. Values taken from ref. 37.

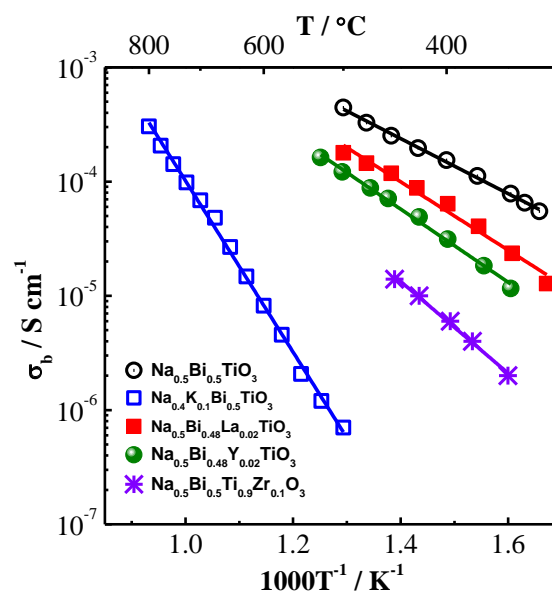


Fig. 4 Arrhenius plot of bulk conductivity,  $\sigma_b$ , of K-, Y-, La- and Zr-doped NBT.

Table 4. Ionic radius, polarisability and bonding strength with oxygen of several possible A-site dopant ions. Data for polarisability (except La<sup>3+</sup>) and bonding strength with oxygen are from refs.38 and 39, respectively.

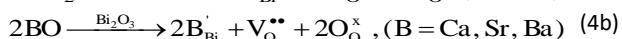
Dopant	Ionic radius (Å)	Polarisability (Å <sup>3</sup> )	Bonding strength with oxygen (kJ·mol <sup>-1</sup> )
Na <sup>+</sup>	1.39 (12-fold)	1.80	257
K <sup>+</sup>	1.64 (12-fold)	3.83	239
Bi <sup>3+</sup>	1.39 (12-fold)	6.12	343
La <sup>3+</sup>	1.36 (12-fold)	4.82 <sup>40</sup>	799
Y <sup>3+</sup>	1.06 (12-fold)	3.81	719
Ti <sup>4+</sup>	0.605 (6-fold)	2.93	672
Zr <sup>4+</sup>	0.72 (6-fold)	3.25	801

#### Acceptor-doping<sup>41-43</sup>

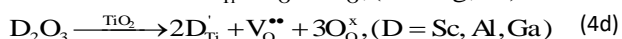
Nominally stoichiometric NBT exhibits high oxide-ion conductivity. It is very promising to develop a family of oxide-ion conductors based on NBT. Enhancement of conductivity can be achieved by inducing a low level of Bi-deficiency in undoped NBT. However, the Bi-deficiency level in NBT is very low. Alternative approaches are required to enhance the oxide-ion conductivity of NBT. Acceptor doping is a commonly employed strategy to enhance ionic conductivity in fluorite-type and perovskite-type oxide-ion conductors by creating oxygen vacancies. In this section, the defect mechanism of acceptor doping in NBT and its effect on the oxide-ion conductivity are reviewed. Acceptor dopants are limited to fix valency metals such as K<sup>+</sup>, Ca<sup>2+</sup>, Sr<sup>2+</sup>, Ba<sup>2+</sup> (to replace Bi<sup>3+</sup> on the A-site) and Mg<sup>2+</sup>, Zn<sup>2+</sup>, Sc<sup>3+</sup>, Al<sup>3+</sup>, Ga<sup>3+</sup> (to replace Ti<sup>4+</sup> on the B-site). Transition metal ions such as Fe<sup>3+</sup>, Co<sup>3+</sup>, Ni<sup>2+</sup> and Mn<sup>3+</sup> on the B-site may introduce electronic conduction into NBT and are therefore not included in this review.

NBT has an ABO<sub>3</sub> perovskite structure where the A-site is shared by randomly distributed Na<sup>+</sup> and Bi<sup>3+</sup> ions and the B-site is occupied by Ti<sup>4+</sup> ions. Depending on the ionic size, acceptor-type dopants can be doped either on the A-site to replace Bi<sup>3+</sup> (larger dopant ions) or on the B-site to replace Ti<sup>4+</sup> (smaller dopant ions). In each case, doping may occur by either an ionic or electronic compensation mechanism. In the case of the former, acceptor doping would create oxygen vacancies. A summary of the defect reactions investigated for a range of A- and B-site acceptor dopants in this study (given in brackets) are described by the following Kroger-Vink equations:

A-site:



B-site:



However, the influence of acceptor-doping on the electrical properties in many perovskite titanates, e.g., BaTiO<sub>3</sub> (BT) and SrTiO<sub>3</sub> (ST) is often more complex with either *n*-type, *p*-type or oxide ion conductivity being dominant depending on a combination of the oxygen-partial-pressure, annealing temperature and cooling rate conditions employed.<sup>44-46</sup> Furnace cooled, acceptor-doped BT and ST ceramics processed in air usually exhibit *p*-type hole conduction (h<sup>•</sup>) based on the uptake of oxygen (on cooling) as given by the following mechanism



View Article Online  
DOI: 10.1039/C7TA09245H

Therefore, acceptor-doping in NBT can either enhance oxide-ion conductivity by creating oxygen vacancies as described by Equation 4 or enhance *p*-type hole conduction as described by Equation 5. Electrical property measurements on 2% Mg-doped and 2% Sr-doped NB<sub>0.49</sub>T show enhanced bulk conductivity, enhanced oxide-ion transport number and higher oxygen diffusion coefficient compared to undoped NB<sub>0.49</sub>T, as listed in Table 5. These electrical properties prove that acceptor-doping of NB<sub>0.49</sub>T on both sites is predominantly by an ionic compensation mechanism to create oxygen vacancies. Acceptor-doping is therefore effective to enhance oxide-ion conduction of NB<sub>0.49</sub>T without introducing any significant electronic contribution.

Based on the above understanding, various acceptor-type dopants have been selected to dope NBT and NB<sub>0.49</sub>T in an attempt to optimise the oxide-ion conductivity in this perovskite. Among all the dopants and doping levels, a maximum enhancement of σ<sub>b</sub> by less than 1 order of magnitude compared to NB<sub>0.49</sub>T is achieved by 2%Sr-doping on the A-site or 1%Mg-doping on the B-site, as shown in Fig. 5. With other dopants and doping levels the bulk conductivity values are all within the shaded region.

Possible reasons for the limited enhancement of bulk conductivity by acceptor-doping in NBT are; 1) a low solid solution limit of these acceptor dopants (typically < 2 at.%) and 2) trapping of oxygen vacancies especially by B-site acceptor dopants, which decreases the mobility of charge carriers.<sup>37</sup> More fundamentally, R. A. De Souza<sup>45</sup> recently reviewed oxygen vacancy diffusion in a wide variety of ABO<sub>3</sub>-type perovskites ranging from ferroelectric dielectrics such as BaTiO<sub>3</sub> and mixed ionic-electronic conductors such as (Ba<sub>0.5</sub>Sr<sub>0.5</sub>)(Co<sub>0.8</sub>Fe<sub>0.2</sub>)O<sub>3-δ</sub> to electrolytes such as (La<sub>0.9</sub>Sr<sub>0.1</sub>)(Ga<sub>0.8</sub>Mg<sub>0.2</sub>)O<sub>2.85</sub>. He reported a surprising result that regardless of the level of oxygen vacancies in these materials, the oxygen vacancy diffusivity is very similar and considered the possibility of a fundamental limit to oxygen-vacancy diffusivity in the ABO<sub>3</sub> perovskite lattice. Using this oxygen vacancy diffusivity limit for cubic perovskites proposed by De Souza, an upper limit for σ<sub>b</sub> of NBT with an oxygen deficiency of 0.025, calculated from Nernst-Einstein equation, is predicted, as shown by the dashed line in Fig. 5. Above 300 °C, the highest bulk conductivity obtained by either Sr- or Mg-doping is consistent with the value calculated from this upper limit, therefore suggesting optimisation of oxide-ion conductivity in the NBT lattice may have been achieved.

Nevertheless, these acceptor-doped NBTs show attractive bulk conductivity. Comparing with the two best known δ-Bi<sub>2</sub>O<sub>3</sub> oxide-ion conductors used in intermediate-temperature solid oxide fuel cells (IT-SOFCs), (BiO<sub>1.5</sub>)<sub>0.8</sub>(ErO<sub>1.5</sub>)<sub>0.2</sub>, 20ESB and (BiO<sub>1.5</sub>)<sub>0.88</sub>(DyO<sub>1.5</sub>)<sub>0.08</sub>(WO<sub>3</sub>)<sub>0.04</sub>, 8D4WSB, although σ<sub>b</sub> of doped NB<sub>0.49</sub>T is initially lower than 20ESB and 8D4WSB, it shows no appreciable degradation with time contrary to the rapid conductivity degradation of 20ESB and 8D4WSB.<sup>42</sup> They also have the advantage over these δ-Bi<sub>2</sub>O<sub>3</sub> phases as a more sustainable (rare-earth free) material. With excellent ionic conductivity, extremely low levels of degradation and reasonable stability in reducing atmospheres<sup>25, 42, 43</sup>, acceptor-doped NBTs can be promising electrolyte materials for IT-SOFCs.

Table 5. Bulk conductivity ( $\sigma_b$ ), oxide-ion transport number ( $t_{\text{ion}}$ ) and tracer diffusion coefficient ( $D^*$ ) of undoped, 2%Mg-doped and 2%Sr-doped  $\text{NB}_{0.49}\text{T}$ .

	$\sigma_b / \text{S cm}^{-1}$			$t_{\text{ion}}$		$D^* / \text{cm}^2 \text{s}^{-1}$
	150 °C	300 °C	500 °C	600 °C	700 °C	632 °C
$\text{NB}_{0.49}\text{T}$ <sup>25</sup>	$2.08 \times 10^{-7}$	$1.19 \times 10^{-4}$	$1.42 \times 10^{-3}$	0.93	0.92	$2.64 \times 10^{-10}$
2%Mg-doped $\text{NB}_{0.49}\text{T}$ <sup>25</sup>	$7.62 \times 10^{-7}$	$2.57 \times 10^{-4}$	$4.06 \times 10^{-3}$	0.98	0.95	$1.17 \times 10^{-8}$
2%Sr-doped $\text{NB}_{0.49}\text{T}$ <sup>42</sup>	$1.44 \times 10^{-6}$	$4.81 \times 10^{-4}$	$5.13 \times 10^{-3}$	0.96	0.94	-

It is worth mentioning that the  $\log_{10} \sigma_b - 1/T$  relationship of undoped and acceptor-doped NBT shows a change in activation energy,  $E_a$  from  $\sim 0.4$  eV above 300 °C to  $\sim 0.9$  eV below 300 °C (Fig. 5). The reason(s) for a change of  $E_a$  around this temperature has not been fully established but the possibility of a change in charge carrier from oxygen ions to electrons, holes or protons has been excluded by previous studies.<sup>41</sup> A plausible explanation for the change of  $E_a$  is the coexistence of rhombohedral (R) and tetragonal (T) phases in the temperature range from 250 to 400 °C, which was revealed by variable temperature neutron diffraction and TEM studies.<sup>41, 42</sup> An estimation of  $\sigma_b$  from the Maxwell model for a two-phase composite showed good agreement with the experimental data of  $\sigma_b$ , suggesting coexistence of R and T phases may be a plausible explanation for the change in  $E_a$  at  $\sim 300$  °C.<sup>42</sup> Other possible reasons for the change of  $E_a$  are dissociation of defect clusters and/or changing of conduction paths associated with the various NBT polymorphs as recently proposed by Meyer and Albe.<sup>47</sup>

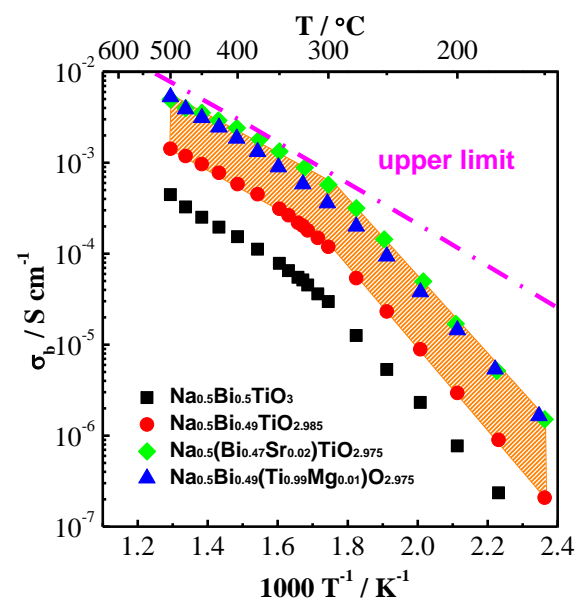


Fig.5 An Arrhenius plot of bulk conductivity,  $\sigma_b$ , for undoped and acceptor-doped NBT ceramics.<sup>41</sup> The dash-dot line represents the upper limit of  $\sigma_b$  based on the oxygen-vacancy diffusion coefficient predicted in ref. 45, see text.

It is interesting to note that many B-site acceptor-doped NBT materials exhibit significantly lower bulk conductivity when compared to A-site acceptor-doped materials with the same nominal oxygen vacancy concentration, Fig. 6. This suggests a strong tendency for the trapping of oxygen vacancies by B-site acceptor dopants, which is supported by first-principle calculations.<sup>37</sup> Trapping of oxygen vacancies decreases their mobility and therefore is detrimental to the oxide-ion conduction. However, it provides an opportunity to control the oxide-ion conduction in NBT using this trapping effect. As the solid solution limit of B-site acceptor dopants in NBT is rather low, some Bi-based high-pressure phases such as  $\text{BiAlO}_3$ ,  $\text{BiGaO}_3$  and  $\text{BiScO}_3$  were used to form solid solutions with NBT to expand the B-site acceptor-dopant level. For example, with  $\text{BiAlO}_3$ , 8%  $\text{Al}^{3+}$  can be incorporated into NBT to replace  $\text{Ti}^{4+}$ <sup>20, 48</sup> compared to < 3% by single B-site doping with  $\text{Al}^{3+}$ . Impedance spectroscopy measurements show a systematic decrease of bulk conductivity with increasing  $x$  in  $(\text{NBT})_{1-x}(\text{BiAlO}_3)_x$  solid solutions, Fig. 7a and electromotive force measurements show a continuous decrease of oxide-ion transport number with increasing  $x$ , Fig. 7b. As incorporation of  $\text{BiAlO}_3$  into NBT does not induce any additional oxygen vacancies or create any additional oxygen ions it can therefore be considered as a 'stoichiometric' doping mechanism.

The suppressed oxide-ion conductivity by  $\text{BiAlO}_3$  incorporation can be attributed mainly to a decrease in oxygen vacancy mobility associated with Al acceptor trapping. A simple calculation suggests 7%  $\text{Al}^{3+}$  can trap all the oxygen vacancies in the solid solution,<sup>48</sup> which is consistent with the  $\sigma_b - x$  and  $t_{\text{ion}} - x$  relationships in Fig. 7. Therefore, using the trapping effect between oxygen vacancies and B-site acceptor dopants, it is possible to fine tune the electrical conduction mechanism from predominant ionic, to mixed ionic-electronic to predominant (but low level) electronic conduction.

To summarise this section, low levels of acceptor-type dopants can be introduced to either the A-site to replace  $\text{Bi}^{3+}$  or to the B-site to replace  $\text{Ti}^{4+}$  to generate oxygen vacancies to enhance the bulk conductivity of NBT. However, the bulk conductivity of acceptor-doped NBT (above 300 °C) seems to approach an upper limit which is restrained by the oxygen vacancy diffusivity in the perovskite lattice. These acceptor-doped NBTs can be promising electrolyte materials for IT-SOFCs. Comparison between A- and B-site dopants suggests that some B-site dopants are more effective at trapping oxygen vacancies to decrease their mobility. This is detrimental for oxide-ion conduction but it provides an opportunity to fine tune the electrical conductivity and conduction mechanism of NBT using the trapping between B-site acceptor dopants and oxygen vacancies to create excellent dielectric materials.

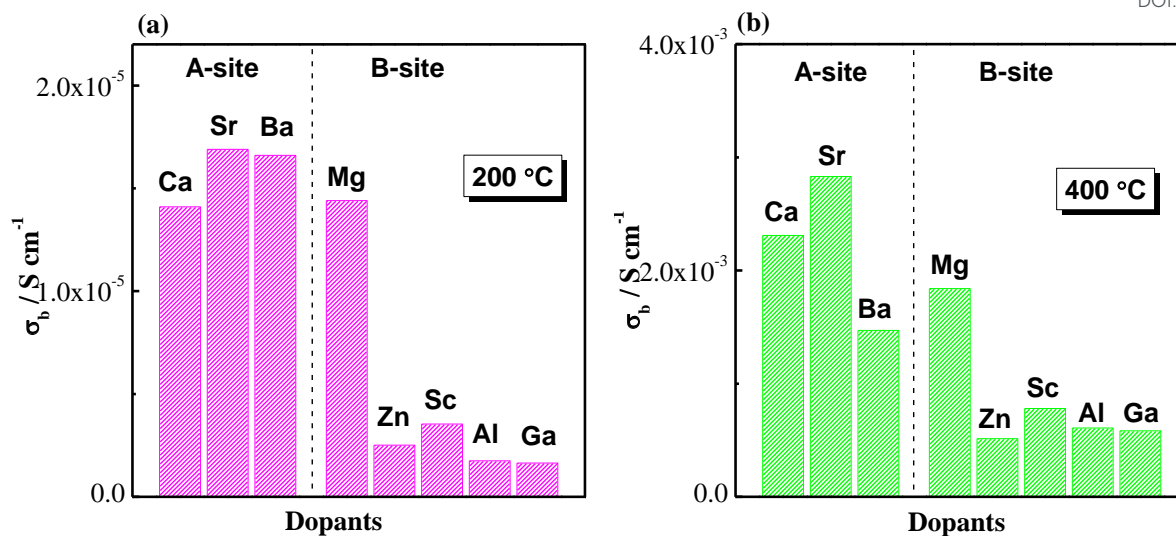


Fig. 6 Comparison of bulk conductivity,  $\sigma_b$ , with A-site and B-site acceptor-dopants at (a) 200 °C and (b) 400 °C.

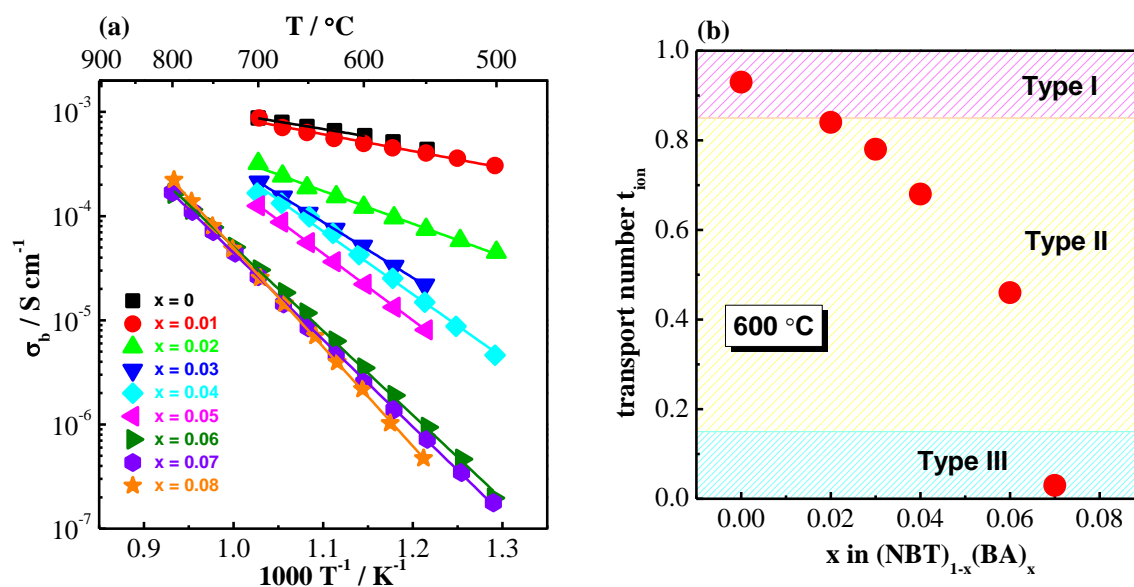
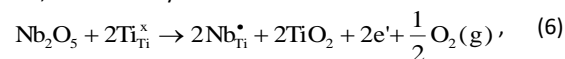


Fig. 7 (a) Arrhenius plots for bulk conductivity and (b) oxide-ion transport number at 600 °C of the  $(\text{NBT})_{1-x}(\text{BiAlO}_3)_x$  ( $0 \leq x \leq 0.08$ ) solid solutions.<sup>48</sup>

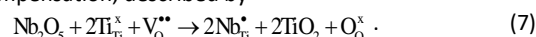
#### Donor-doping<sup>29,34</sup>

Donor-dopants such as Nb can be incorporated into NBT to replace Ti on the B-site. The doping limit of Nb in  $\text{Na}_{0.5}\text{Bi}_{0.5}\text{Ti}_{1-x}\text{Nb}_x\text{O}_{3+0.5x}$  is low with the presence of small amounts of  $\text{Bi}_2\text{Ti}_2\text{O}_7$ - or  $\text{Na}_{0.5}\text{Bi}_{4.5}\text{Ti}_4\text{O}_{15}$ -related secondary phases for  $x \geq 0.02$ .<sup>34</sup> However, extremely low levels of Nb doping can significantly change the electrical conductivity and conduction mechanism of NBT, as summarised below.

When Nb is introduced to replace Ti in NBT, there are at least two possible compensation mechanisms: a) electronic compensation, described by



or b) ionic compensation, described by



The electronic compensation mechanism is commonly adopted by BT or ST-based perovskites, which induces high levels of *n*-type semiconductivity to the materials. For example, Nb doping on the Ti-site can transform BT from a dielectric material to an *n*-type semiconductor with room temperature conductivity  $> 0.01 \text{ S cm}^{-1}$ ;<sup>49</sup>

10 % Nb-doped ST can achieve an electronic conductivity of  $\sim 500 \text{ S cm}^{-1}$ ,<sup>50</sup> which makes it a promising oxide-based thermoelectric material. However, the fact that Nb-doping reduces the bulk conductivity of NBT significantly (Fig. 8) indicates the electronic compensation mechanism is not applicable to NBT. This is attributed to the different band structure of NBT compared with BT or ST. NBT has a high conduction band minimum (ECB) and a high valence band maximum (EVB),<sup>44</sup> which makes it less favourable for electronic donor-doping. Therefore, Nb-doping in NBT occurs via an ionic compensation mechanism described by Equation (6). The excess positive charge from  $\text{Nb}^{5+}$  ions is compensated by filling oxygen vacancies with oxygen. As a result, the oxide-ion conductivity is suppressed due to a decrease in the charge carrier concentration. Consequently the ionic transport number,  $t_{\text{ion}}$ , decreases from 0.93 for NBT to 0.57 for 0.2 at.% Nb-doping, further down to 0.47 for 0.3 at.% Nb-doping and finally below 0.1 for  $\geq 0.5$  at.% Nb-doping (Table 6).

The continuous decrease in oxide-ion conduction in NBT by Nb doping originates from a decrease in the number of oxygen vacancies. It is expected that similar effects can be observed by Ta-, Mo- and W-doping. This mechanism is different from the NBT-BiAlO<sub>3</sub> solid solutions where the suppression of oxide-ion conduction is attributed to a decrease in the oxygen vacancy mobility via trapping by the acceptor-dopants.

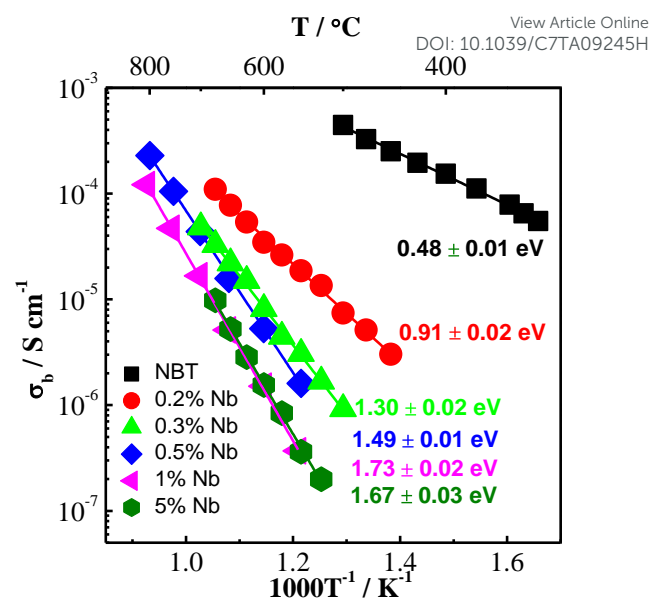


Fig. 8 Arrhenius plot of bulk conductivity,  $\sigma_b$ , of Nb-doped NBT with nominal composition  $\text{Na}_{0.5}\text{Bi}_{0.5}\text{Ti}_{1-x}\text{Nb}_x\text{O}_{3+0.5x}$ . Activation energy for each composition is indicated in the figure. Replotted after refs. 29 and 34.

Table 6. Oxide-ion transport number at 600 – 800 °C, dielectric loss at 600 °C and electrical behaviour of Nb-doped NBT at various doping levels.

Doping level (%)	Nominal composition	$t_{\text{ion}}$			tan $\delta$ at 600 °C	Type
		600 °C	700 °C	800 °C		
0	$\text{Na}_{0.5}\text{Ti}_{0.5}\text{TiO}_3$ <sup>25</sup>	0.93	0.93	0.85	$\gg 0.2$	I
0.2	$\text{Na}_{0.5}\text{Bi}_{0.5}\text{Ti}_{0.998}\text{Nb}_{0.002}\text{O}_{3.001}$ <sup>29</sup>	0.57	0.63	0.63	0.083	II
0.3	$\text{Na}_{0.5}\text{Bi}_{0.5}\text{Ti}_{0.997}\text{Nb}_{0.003}\text{O}_{3.0015}$ <sup>29</sup>	0.47	0.49	0.53	0.016	II
0.5	$\text{Na}_{0.5}\text{Bi}_{0.5}\text{Ti}_{0.995}\text{Nb}_{0.005}\text{O}_{3.0025}$ <sup>30</sup>	0.06	0.06	0.06	$< 0.01$	III
1	$\text{Na}_{0.5}\text{Bi}_{0.5}\text{Ti}_{0.99}\text{Nb}_{0.01}\text{O}_{3.005}$ <sup>31</sup>	Not available			$< 0.01$	III
5	$\text{Na}_{0.5}\text{Bi}_{0.5}\text{Ti}_{0.95}\text{Nb}_{0.05}\text{O}_{3.025}$ <sup>29</sup>	0.04	0.03	0.03	$< 0.01$	III

## Concluding remarks

The ferroelectric perovskite NBT can present three types of electrical behaviour based on oxide-ion conduction (Type I), mixed ionic-electronic conduction (Type II) and insulator/dielectric (Type III) by controlling the defects introduced by various mechanisms. The flexibility in fine tuning the electrical properties of NBT make it an attractive material to be applied in various technologically important devices such as SOFCs (Type I) and electronic components such as capacitors and piezoelectric sensors/actuators (Type III). To date, the major findings include:

- 1) The A-site Na or Bi non-stoichiometry level in NBT is very low. The electrical conductivity of NBT is dependent on the

starting Na/Bi ratio. Based on our current processing conditions Na/Bi  $\geq 1$  is required to obtain high oxide-ion conductivity. Na/Bi  $< 1$  switches the electrical conduction mechanism from predominant oxide-ion conduction to predominant (but low level) electronic conduction. NBT ceramics with a considerable amount of Bi-rich secondary phase can exhibit mixed ionic-electronic conduction.

- 2) The local configuration at the saddle point is critical to the oxide-ion conduction in NBT. Polarisability and bonding strength with oxygen of the cations, especially the latter, are the most important factors that influence the oxide-ion migration. Due to the high polarisability and weak Bi-O bond, it can be predicted that most isovalent dopants on

the A-site to replace Bi<sup>3+</sup> are detrimental to the oxide-ion conduction.

- 3) Low levels of acceptor dopants can be introduced to either the A-site to replace Bi<sup>3+</sup> or to the B-site to replace Ti<sup>4+</sup> to create oxygen vacancies and consequently enhance the oxide-ion conductivity. Acceptor-doped NBTs have high oxide-ion conductivity, extremely low levels of conductivity degradation and reasonable stability in reducing atmospheres (at least below 550 °C) and are therefore promising electrolyte materials for IT-SOFCs. Comparison between A- and B-site dopants suggests a stronger tendency for trapping of oxygen vacancies by B-site acceptor-dopants. Using this trapping effect, it is possible to control the level of oxide-ion conduction and therefore fine-tune the electrical conductivity and conduction mechanism of NBT according to the requirements of different applications.
- 4) Low levels of donor-dopants can be introduced at the B-site to replace Ti<sup>4+</sup>. Donor doping fills the oxygen vacancies in NBT and therefore suppresses the oxide-ion conductivity. Depending on the doping level, NBT can present mixed ionic-electronic conduction (Type II) and finally insulating/dielectric behaviour based on a low level of electronic conduction (Type III).

### Conflicts of interest

There are no conflicts to declare.

### Acknowledgements

We thank the EPSRC for funding EP/L027348/1. E. Pradal-Velázquez thanks CONACYT for his scholarship under "Becas CONACYT al extranjero (registro 327115)".

### References

- 1 E. Aksel, J. L. Jones, *Sensors*, 2010, **10**, 1935.
- 2 D. Damjanovic, N. Klein, J. Lin, V. Porokhonsky, *Funct. Mater. Lett.*, 2010, **3**, 5.
- 3 K. Reichmann, A. Feteira, M. Li, *Materials*, 2015, **8**, 8467.
- 4 M. Davies, E. Aksel, J. L. Jones, *J. Am. Ceram. Soc.*, 2011, **94**, 1314.
- 5 G. O. Jones, P. A. Thomas, *Acta Cryst. B*, 2002, **58**, 168.
- 6 S. Gorfman, P. A. Thomas, *J. Appl. Crystallogr.*, 2010, **43**, 1409.
- 7 E. Aksel, J. S. Forrester, J. L. Jones, P. A. Thomas, K. Page, M. R. Suhomel, *Appl. Phys. Lett.*, 2011, **98**, 152901.
- 8 I. Levin and I. M. Reaney, *Adv. Funct. Mater.*, 2012, **22**, 3445.
- 9 B. N. Rao, R. Datta, S. S. Chandrashekar, D. K. Mishra, V. Sathe, A. Senyshyn, R. Ranjan, *Phys. Rev. B*, 2013, **88**, 224103.
- 10 E. Aksel, J. S. Forrester, B. Kowalski, P. A. Thomas, J. L. Jones, *Appl. Phys. Lett.*, 2011, **99**, 222901.
- 11 E. Aksel, H. Foronda, K. Calhoun, J. L. Jones, S. Schaab, T. Granzow, *Funct. Mater. Lett.*, 2010, **3**, 45.
- 12 E. Aksel, E. Erdem, P. Jakes, J. L. Jones and R. A. Eichel, *Appl. Phys. Lett.*, 2010, **97**, 012903.
- 13 E. Aksel, J. S. Forrester, B. Kowalski, M. Deluca, D. Damjanovic, J. L. Jones, *Phys. Rev. B*, 2012, **85**, 024121.
- 14 D. Q. Xiao, D. M. Lin, J. G. Zhu, P. Yu, *J. Electroceram.*, 2008, **21**, 34.
- 15 T. Takenaka, K. Maruyama and K. Sakata, *Jpn. J. Appl. Phys.*, 1991, **30**, 2236. DOI: 10.1039/C7TA09245H
- 16 J. R. Gomah-Petry, S. Said, P. Marchet, J. P. Mercurio, *J. Eur. Ceram. Soc.*, 2004, **24**, 1165.
- 17 E. Venkata Ramana, B. V. Bahuguna Saradhi, S. V. Suryanarayana, T. Bhima Sankaram, *Ferroelectrics*, 2005, **324**, 55.
- 18 Y. Hiruma, K. Yoshii, H. Nagata, T. Takenaka, *Ferroelectrics*, 2007, **346**, 114.
- 19 Y. Hiruma, H. Nagata, T. Takenaka, *J. Appl. Phys.*, 2008, **104**, 124106.
- 20 H. Yu, Z. Ye, *Appl. Phys. Lett.*, 2008, **93**, 112902.
- 21 Y. Hiruma, H. Nagata, T. Takenaka, *J. Appl. Phys.*, 2009, **105**, 084112.
- 22 Y. S. Sung, J. M. Kim, J. H. Cho, T. K. Song, M. H. Kim, H. H. Chong, T. G. Park, D. Do, S. S. Kim, *Appl. Phys. Lett.*, 2010, **96**, 022901.
- 23 Y. S. Sung, J. M. Kim, J. H. Cho, T. K. Song, M. H. Kim, T. G. Park, *Appl. Phys. Lett.*, 2011, **98**, 012902.
- 24 H. Nagata, *J. Ceram. Soc. Jpn.*, 2008, **116**, 271.
- 25 M. Li, M. J. Pietrowski, R. A. De Souza, H. Zhang, I. M. Reaney, S. N. Cook, J. A. Kilner, D. C. Sinclair, *Nat. Mater.*, 2014, **13**, 31.
- 26 M. Li, H. Zhang, S. N. Cook, L. Li, J. A. Kilner, I. M. Reaney, D. C. Sinclair, *Chem. Mater.*, 2015, **27**, 629.
- 27 D. Schütz, M. Deluca, W. Krauss, A. Feteira, T. Jackson, K. Reichmann, *Adv. Funct. Mater.*, 2012, **22**, 2285.
- 28 M. Bousquet, J. -R. Duclère, E. Orhan, A. Boule, C. Bachelet, C. Champeaux, *J. Appl. Phys.*, 2010, **107**, 104107.
- 29 L. Li, M. Li, H. Zhang, I. M. Reaney, D. C. Sinclair, *J. Mater. Chem. C*, 2016, **4**, 5779.
- 30 L. Li, Oxide ion conduction in A-site Bi-containing perovskite-type ceramics, PhD Thesis, University of Sheffield, 2016.
- 31 P. Wu, D. C. Sinclair, unpublished results.
- 32 F. Yang, D. C. Sinclair, unpublished results.
- 33 L. Li, F. Yang, E. Pradal-Venazquez, D. C. Sinclair, unpublished results.
- 34 M. Li, L. Li, J. Zang, D. C. Sinclair, *Appl. Phys. Lett.*, 2015, **106**, 102904.
- 35 M. S. Islam, *J. Mater. Chem.* 2000, **10**, 1027.
- 36 J. A. Dawson, H. Chen, I. Tanaka, *J. Mater. Chem. A*, 2015, **3**, 16574.
- 37 X. He, Y. Mo, *Phys. Chem. Chem. Phys.*, 2015, **17**, 18035.
- 38 N. M. Gimes, R. W. Grimes, *J. Phys. Condes. Matter*, 1998, **10**, 3029.
- 39 Y. R. Luo, *Compressive Handbook of Chemical Bond Energies*, CRC Press, Boca Raton, FL, 2017.
- 40 C. Vineis, P. K. Davies, T. Negas, S. Bell, *Mater. Res. Bull.*, 1996, **31**, 431.
- 41 F. Yang, M. Li, L. Li, P. Wu, E. Pradal-Velázquez, D. C. Sinclair, *J. Mater. Chem. A* DOI: 10.1039/c7a07667c.
- 42 F. Yang, H. Zhang, L. Li, I. M. Reaney, D. C. Sinclair, *Chem. Mater.*, 2016, **28**, 5269.
- 43 F. Yang, P. Wu, D. C. Sinclair, *Solid State Ionics*, 2017, **299**, 38.
- 44 S. Li, J. Morasch, A. Klein, C. Chirila, L. Pintilie, L. Jia, K. Ellmer, M. Naderer, K. Reichmann, M. Gröting, K. Albe, *Phys. Rev. B*, 2013, **88**, 045428.
- 45 R. A. De Souza, *Adv. Funct. Mater.*, 2015, **25**, 6326.
- 46 D. M. Symth, *J. Electroceram.*, 2003, **11**, 89.
- 47 K-C. Meyer, K. Albe, *J. Mater. Chem. A*, 2017, **5**, 4368.
- 48 F. Yang, P. Wu, D. C. Sinclair, *J. Mater. Chem. C*, 2017, **5**, 7243.
- 49 B. Huybrechts, K. Ishizaki, M. Takata, *J. Mater. Sci.*, 1995, **30**, 2463.
- 50 B. Zhang, J. Wang, T. Zou, S. Zhang, X. Yaer, N. Ding, C. Liu, L. Miao, Y. Li, Y. Wu, *J. Mater. Chem. C*, 2015, **3**, 11406.